JACS
JOURNAL OF THE AMERICAN CHEMICAL SOCIETY

Communication

pubs.acs.org/JACS

Patchy Supramolecules as Versatile Tools To Probe Hydrophobicity in Nanoglobular Systems

Luis M. Negrón, Yazmary Meléndez-Contés, and José M. Rivera*

Department of Chemistry, University of Puerto Rico, Río Piedras Campus, Río Piedras, Puerto Rico 00931

Ⓢ *Supporting Information*

ABSTRACT: We describe precise supramolecules that enable the evaluation of the effective hydrophobicity of amphiphilic or "patchy" nanoglobular systems. These supramolecules exhibit the lower critical solution temperature phenomenon, which provides a quantitative measure of their effective hydrophobicity. Specifically, two isomeric 8-aryl-2′-deoxyguanosine derivatives with a transposed pair of methylene groups self-assemble into hexadecameric nanoglobular supramolecular G-quadruplexes (SGQs) that show large differences in their transition temperatures as determined by turbidity and differential scanning calorimetry studies. Molecular modeling studies suggested that differential clustering of the hydrophobic patches on the surface is responsible for the striking differences between the two isomeric supramolecules.

The juxtaposition of hydrophobic and hydrophilic regions (patches) on the surface of proteins plays a pivotal role in both health and disease.[1] For example, hydrophobic patches on the surface of proteins mediate protein−protein interactions and have provided a means for the evolution of multimeric systems.[2] Conversely, the emergence of a hydrophobic patch on a mutant hemoglobin results in detrimental polymerization leading to sickle cell anemia.[3] However, despite its long and interesting history[4] in addition to recent seminal findings,[5] critical details regarding the hydrophobic effect have yet to be elucidated, such as in the context of the rough amphiphilic (patchy) surfaces on precise nanoglobular systems, including many soluble proteins.[6]

The development of model systems with patchy or amphiphilic surfaces has the potential to clarify some of those details and also to enable technological applications.[7] A number of model systems such as polymers or micelles could be envisioned to address this challenge. However, they have multiple limitations such as their polydispersity and the difficulty of precisely controlling their composition and structure. Here we describe a family of hexadecameric nanoglobular supramolecular G-quadruplexes (SGQs) with precise structures and amphiphilic "patchy" surfaces that offer a complement to polymeric systems (Figure 1).[8] These systems are thermoresponsive [i.e., they show the lower critical solution temperature (LCST) phenomenon], which gives us a quantitative measure of their effective hydrophobicity.[9] We demonstrate that the distribution of the patches can in fact be used to modulate the transition temperature for the onset of the LCST phenomenon and thus their hydrophobicity.

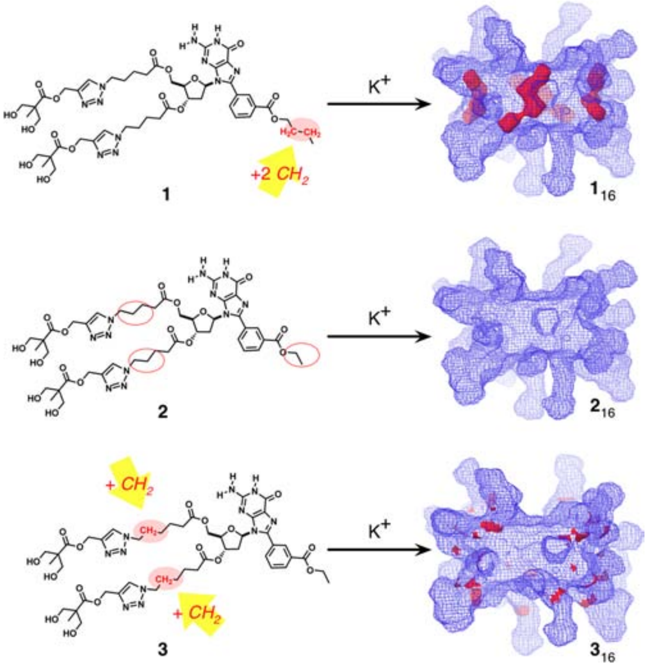

Figure 1. Kekulé structures for **1**, **2**, and **3**. Addition of two methylene groups (red) to **2** (control) produces the structural isomers **1** with two methylenes in the aryl group and **3** with one methylene in each side chain attached to the ribose. Addition of KI in aqueous solution generates self-assembled nanoglobules ($\mathbf{1}_{16}$, $\mathbf{2}_{16}$, and $\mathbf{3}_{16}$) with patchy surfaces. The models on the right represent the solvent-accessible surface areas of the SGQs with the methylenes highlighted in red. They were generated using Maestro after minimizations in MacroModel with the AMBER 94 force field.[10]

Compounds **1**, **2**, and **3** were prepared using the methodology described previously for this family of compounds (Figure S1 in the Supporting Information).[11−13] In aqueous phosphate-buffered solutions (pH 7.4, 2 M KI), all three compounds (10 mM) showed signature peaks in the ^{1}H NMR spectra confirming the formation of the corresponding hexadecamers $\mathbf{1}_{16}$, $\mathbf{2}_{16}$, and $\mathbf{3}_{16}$ (Figures S18−S20).[13] Turbidity experiments (transmittance at 500 nm) confirmed the thermoresponsive behavior of these SGQs and provided the first indication that the different patchy surfaces indeed impact their effective hydrophobicities (Figure 2). The cloud-point temperature (T_{cp}) for $\mathbf{1}_{16}$ was 10 °C, while T_{cp} = 32 °C for its

Received: February 6, 2013
Published: February 25, 2013

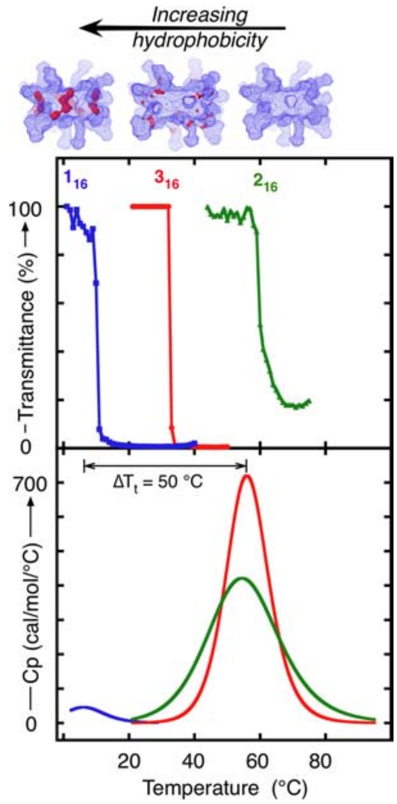

Figure 2. (top) Turbidity curves (measured at 500 nm) and (bottom) DSC endotherms for $\mathbf{1}_{16}$ (blue), $\mathbf{2}_{16}$ (green), and $\mathbf{3}_{16}$ (red).[12] The measurements were performed in aqueous phosphate-buffered solutions (10 mM in **1**−**3**, pH 7.4, 2 M KI).

isomer $\mathbf{3}_{16}$ and 60 °C for $\mathbf{2}_{16}$.[14] These results suggest that $\mathbf{1}_{16}$ is substantially more hydrophobic than $\mathbf{3}_{16}$ ($\Delta T_{cp} \approx 22$ °C), while $\mathbf{2}_{16}$ appears to be the least hydrophobic of all.[15] The turbidity above T_{cp} resulted from the formation of a colloidal suspension of microglobules, which were shown by dynamic light scattering (DLS) to have average hydrodynamic diameters (D_H) in the range between 4.5 and 21.7 μm (Figures S25 and S26).[11,16]

Differential scanning calorimetry (DSC) experiments provided further support of the turbidity measurements while revealing additional data associated with the thermodynamic parameters of these SGQs (Figures S23−S25).[13] After data deconvolution, the DSC endotherms revealed two different processes: the transition temperature (T_t) corresponding to the LCST and, at higher temperatures, the melting temperature (T_m) of the SGQs within the microglobules (Figures S23−S25).[13] The endotherms for $\mathbf{1}_{16}$ and $\mathbf{3}_{16}$ showed maxima corresponding to T_t values of 6.4 and 56.2 °C, respectively ($\Delta T_t \approx 50$ °C), while that for $\mathbf{2}_{16}$ (with two fewer methylene groups per subunit) showed a T_t of ~55.0 °C (Table 1). Furthermore, these measurements revealed that these systems have T_m values in the range 59−70 °C, with $\mathbf{1}_{16}$ being the least thermally stable of the three assemblies. This is likely the result of its larger steric bulk imposed by the butoxy group near the core of the assembly (vs ethoxy in **2** and **3**; Figure 1).

Higher T_t values relate to the energy required to expel the associated water molecules, while the corresponding enthalpy (ΔH_t) indicates the number of water molecules associated within the hydration shells. For example, the fact that there are fewer water molecules of hydration associated with $\mathbf{1}_{16}$ is reflected in the lower magnitude of the enthalpy for the process (0.75 kcal/mol) compared with the corresponding values for $\mathbf{2}_{16}$ and $\mathbf{3}_{16}$ (~12 kcal/mol) (Figure 2 and Table 1). The apparent large discrepancy between the onset of turbidity (T_{cp}) and the maximum of the DSC peak (T_t) for $\mathbf{3}_{16}$ results from an athermal association process between the nanoglobular assemblies that is likely mediated by interactions between the peripheral hydroxyl groups and water molecules. This phenomenon is similar to the one reported by Winnik and co-workers[17] using telechelic poly(*N*-isopropylacrylamide) (PNIPAM) derivatives that form micellar assemblies. According to Winnik, this water-mediated association (of micelles, in their case) leads to globules that are large enough to scatter light (thus the onset of turbidity), but since it does not involve partitioning of the water molecules of hydration to the bulk, it seems to be below the detection limit of the calorimeter. The fact that this occurs exclusively with $\mathbf{3}_{16}$ (since for the other two assemblies the onset of turbidity occurs slightly above T_t) will be the subject of future molecular dynamics studies aimed at illuminating this particular phenomenon.

Table 1. Thermodynamic Parameters for Supramolecules $\mathbf{1}_{16}$, $\mathbf{2}_{16}$, and $\mathbf{3}_{16}$ Obtained from Turbidity and DSC measurements

SGQ	T_{cp} (°C)[a]	T_t (°C)[b]	T_m (°C)[c]	ΔH_t (kcal/mol)
$\mathbf{1}_{16}$	10	6.35 ± 0.03	59.50 ± 0.03	0.75 ± 0.04
$\mathbf{2}_{16}$	60	55.1 ± 0.4	68.4 ± 0.1	12.2 ± 0.5
$\mathbf{3}_{16}$	32	56.19 ± 0.06	69.98 ± 0.05	12.4 ± 0.1

[a] Cloud-point temperature as determined by turbidity measurements. [b] Transition temperature as determined by DSC. [c] Melting temperature as determined by DSC.

Molecular modeling studies of these SGQs provided vital clues to help explain why $\mathbf{1}_{16}$ shows a significantly higher hydrophobicity than its isomer $\mathbf{3}_{16}$ (Figure 1). The former shows clusters of patches concentrated around the core's surface, while the latter presents a more scattered distribution of such patches. These smaller and more distributed patches on the surface of $\mathbf{3}_{16}$ can be accommodated in the tetrahedral water network with minimal disruption of the hydrogen bonds. Interestingly, this remodeling of the patches on the surface of $\mathbf{3}_{16}$ has an effect very similar to the actual removal of the hydrophobic patches ($\mathbf{2}_{16}$). While the distribution of patches enables the formation of clusters of $\mathbf{3}_{16}$ at lower temperatures (i.e., lower T_{cp}) relative to $\mathbf{2}_{16}$, the former shows T_t and ΔH_t values very similar to those of the latter, although the sharper endotherm transition for $\mathbf{3}_{16}$ (Figure 2) hints at a more cooperative dehydration process. These results underscore the importance of having systems that are modular and molecularly precise, which could enable future molecular dynamics studies to illuminate these phenomena further.

The hydrophobic effect never ceases to provide surprising twists in its manifestations. Although much progress has been made since its first descriptions in the early 20th century,[4] it remains a fertile ground for new discoveries and applications. We have demonstrated an additional use for SGQs in the elaboration of useful tools for studying the hydrophobic effect in a precise nanoglobular system. We have shown how the three-dimensional distribution of hydrophobic elements leads to a profound impact on the hydrophobicity of the assembly. We expect these results to enable further studies on the dynamics of water molecules in contact with patchy surfaces having different sizes and shapes, which should complement studies performed with polymers. For example, related systems should enable the evaluation of how the specific nature of the patches (e.g., saturated versus unsaturated) in conjunction with their relative sizes and distributions affect the hydrophobicity. We believe that the modularity of the system will aid both experimental and theoretical approaches aimed at answering these and related questions.

■ ASSOCIATED CONTENT

Ⓢ Supporting Information

Detailed synthetic procedures, characterization data for all new compounds, experimental protocols, and NMR data. This material is available free of charge via the Internet at http://pubs.acs.org.

■ AUTHOR INFORMATION

Corresponding Author

riveralab.upr@gmail.com

Notes

The authors declare no competing financial interest.

■ ACKNOWLEDGMENTS

We thank NIH-SCORE (Grant 5SC1GM093994) and the RISE Program (Grant 5R25GM061151) for financial support. L.M.N. thanks the Alfred P. Sloan Foundation RISE Program for graduate fellowships. We are also grateful to Dr. Irving E. Vega and Edwin Vazquez-Rosa for assistance with mass spectrometry measurements.

■ REFERENCES

(1) (a) Ball, P. *Nature* **2011**, *478*, 467−468. (b) Ball, P. *Chem. Rev.* **2008**, *108*, 74−108.

(2) (a) Levy, E. D.; Boeri Erba, E.; Robinson, C. V.; Teichmann, S. A. *Nature* **2008**, *453*, 1262−1265. (b) Tsai, C. J.; Nussinov, R. *Protein Sci.* **1997**, *6*, 1426−1437.

(3) Galkin, O.; Vekilov, P. G. *J. Mol. Biol.* **2004**, *336*, 43−59.

(4) Tanford, C. *Protein Sci.* **1997**, *6*, 1358−1366.

(5) For selected examples related to the hydrophobic effect, see: (a) Li, I. T. S.; Walker, G. C. *Acc. Chem. Res.* **2012**, *45*, 2011−2021. (b) Patel, A. J.; Varilly, P.; Jamadagni, S. N.; Acharya, H.; Garde, S.; Chandler, D. *Proc. Natl. Acad. Sci. U.S.A.* **2011**, *108*, 17678−17683. (c) Garde, S.; Patel, A. J. *Proc. Natl. Acad. Sci. U.S.A.* **2011**, *108*, 16491−16492. (d) Li, I. T. S.; Walker, G. C. *Proc. Natl. Acad. Sci. U.S.A.* **2011**, *108*, 16527−16532. (e) Jamadagni, S. N.; Godawat, R.; Dordick, J. S.; Garde, S. *J. Phys. Chem. B* **2009**, *113*, 4093−4101. (f) Giovambattista, N.; Lopez, C. F.; Rossky, P. J.; Debenedetti, P. G. *Proc. Natl. Acad. Sci. U.S.A.* **2008**, *105*, 2274−2279. (g) Giovambattista, N.; Debenedetti, P. G.; Rossky, P. J. *J. Phys. Chem. C* **2007**, *111*, 1323−1332. (h) Chandler, D. *Nature* **2005**, *437*, 640−647. (i) Lum, K.; Chandler, D.; Weeks, J. D. *J. Phys. Chem. B* **1999**, *103*, 4570−4577.

(6) Granick, S.; Bae, S. *Science* **2008**, *322*, 1477−1478.

(7) (a) Glotzer, S. C.; Solomon, M. J. *Nat. Mater.* **2007**, *6*, 557−562. (b) Zhang, Z.; Glotzer, S. C. *Nano Lett.* **2004**, *4*, 1407−1413.

(8) For examples of supramolecular systems in aqueous environments, see: (a) Gibb, B. C. *Nat. Chem.* **2010**, *2*, 512−513. (b) Uhlenheuer, D. A.; Petkau, K.; Brunsveld, L. *Chem. Soc. Rev.* **2010**, *39*, 2817−2826. (c) Zayed, J. M.; Nouvel, N.; Rauwald, U.; Scherman, O. A. *Chem. Soc. Rev.* **2010**, *39*, 2806−2816. (d) Oshovsky, G. V.; Reinhoudt, D. N.; Verboom, W. *Angew. Chem., Int. Ed.* **2007**, *46*, 2366−2393.

(9) (a) Urry, D. W. *J. Phys. Chem. B* **1997**, *101*, 11007−11028. (b) Urry, D. W.; Gowda, D. C.; Parker, T. M.; Luan, C. H.; Reid, M. C.; Harris, C. M.; Pattanaik, A.; Harris, R. D. *Biopolymers* **1992**, *32*, 1243−1250.

(10) (a) *MacroModel*, version 9.5; Schrödinger, LLC: New York, 2007. (b) *Maestro*, version 8.0.315; Schrödinger, LLC: New York, 2007.

(11) (a) Betancourt, J. E.; Rivera, J. M. *J. Am. Chem. Soc.* **2009**, *131*, 16666−16668. (b) Betancourt, J. E.; Subramani, C.; Serrano-Velez, J. L.; Rosa-Molinar, E.; Rotello, V. M.; Rivera, J. M. *Chem. Commun.* **2010**, *46*, 8537−8539.

(12) Monomers **1** and **2** (Figure 1) were synthesized as previously reported for **3** (see ref 11; Figure S1). All of the data for **3**, including its self-assembly and LCST properties, were previously reported in ref 11b.

(13) See the Supporting Information.

(14) The values of T_t for these SGQs showed no significant changes as a function of concentration over the range 5−10 mM.

(15) Cooling all of the SGQs below their respective T_t ($\mathbf{1}_{16}$ to 0 °C; $\mathbf{2}_{16}$ and $\mathbf{3}_{16}$ to 25 °C) reestablished the initial state of solubility with fairly transparent solutions. Furthermore, the process could be repeated at least seven times for each sample with little sign of fatigue (Figures S21 and S22).

(16) Below T_t, the D_H values were 3.6−4.0 nm for $\mathbf{1}_{16}$, 4.0−4.6 nm for $\mathbf{2}_{16}$, and 5 nm for $\mathbf{3}_{16}$.

(17) (a) Obeid, R.; Tanaka, F.; Winnik, F. M. *Macromolecules* **2009**, *42*, 5818−5828. (b) Kujawa, P.; Segui, F.; Shaban, S.; Diab, C.; Okada, Y.; Tanaka, F.; Winnik, F. M. *Macromolecules* **2006**, *39*, 341−348.